STARflo™: A Suprachoroidal Drainage Implant Made from STAR® Biomaterial

22

Sayeh Pourjavan, Nathalie J.M. Collignon, Veva De Groot, Rich A. Eiferman, Andrew J. Marshall, and Cecile J. Roy

Introduction

Aqueous humor is produced in the posterior chamber of the eye by the ciliary body epithelium at a relatively constant rate of about 2.5 µl/min and flows into the anterior chamber, passing around the lens and through the pupillary opening in the iris. It is a complex mixture of electrolytes, organic solutes, growth factors, and other proteins that supply nutrients to the nonvascularized tissues of the anterior chamber (i.e., trabecular meshwork, lens, and corneal endothelium). Egress of aqueous humor from the anterior chamber occurs via two distinct pathways: conventional and uveoscleral. In the primary (conventional) outflow pathway, accounting for the majority of the aqueous outflow in normal individuals, aqueous humor passes through the trabecular meshwork, enters a space lined with endothelial cells (Schlemm's canal), and drains into collector channels and then into the aqueous veins. The uveoscleral outflow pathway, which may account for 10–60 % of total flow in the human eye [1–4], comprises the interstitium of the ciliary body, the suprachoroidal space, and, ultimately, the choroidal and scleral vasculature. Elevated intraocular pressure (IOP) typically results from increased resistance or compromise in either or both outflow pathway.

While research is investigating ways to protect the optic nerve and the vision from an elevated pressure, the only therapeutic approach currently available in glaucoma is to reduce the intraocular pressure. Glaucoma surgery is intended to reduce the IOP when the target IOP cannot be reached with maximal medical therapy or laser treatment. Due to complications with established surgical approaches such as trabeculectomy (early hypotony, blebitis, endophthalmitis, shallow anterior chamber, etc.) and closure by the body's natural healing process, a variety of seton devices, including aqueous shunts, are in use or being evaluated as alternative surgical treatments for patients with glaucoma. Glaucoma drainage devices (GDDs) aim at creating an alternate aqueous pathway from the anterior chamber by channeling aqueous humor out of the eye, hence reducing IOP. Traditionally, GDDs have been developed to provide an artificial conduit (small tube) for aqueous humor to travel from the anterior chamber and spread across a subconjunctivally located plate to form a filtering bleb [5, 6]. Although this filtration is nonphysiologic, the traditional tube shunts can effectively reduce IOP. However, they share similar postoperative challenges with trabeculectomy including bleb leakage, overfiltration, bleb dysesthesia, bleb encapsulation, and fibrosis. They also have their own unique set of postoperative risks, such as corneal endothelial cell death, ptosis, diplopia, tube migration, tube or plate exposure, and tube lumen occlusions. As a result,

S. Pourjavan, MD, PhD
Department of Ophthalmology, Cliniques Universitaires St. Luc, UCL, Avenue Hippocrate 10, Brussels 1100, Belgium
e-mail: sayehpourjavan@hotmail.com

N.J.M. Collignon, MD, PhD
Division of Neuro-Ophthtalmology and Glaucoma, Department of Ophthalmology, University Hospital of Liège, Domaine du Sart Tilman B35 avenue de l'hôpital 1, avenue de l'hôpital 1, Liège 4000, Belgium
e-mail: nathalie.collignon@chu.ulg.ac.be

V. De Groot, MD, PhD
Department of Ophthalmology, University Hospital Antwerp, Edegem, Belgium
e-mail: Veva.DeGroot@uza.be

R.A. Eiferman, MD, FACS
Department of Ophthalmology, University of Louisville, 6400 Dutchmans Pkwy, Louisville, KY 40205, USA
e-mail: reiferman@cs.com

A.J. Marshall, PhD
Healionics Corporation, 2121 N 35th St, Seattle, WA 98103, USA
e-mail: andrewm@healionics.com

C.J. Roy, PhD (✉)
iSTAR Medical SA, Rue Phocas Lejeune 25/3, Isnes 5032, Belgium
e-mail: cecile@istarmed.com

Electronic supplementary material Supplementary material is available in the online version of this chapter at http://dx.doi.org/10.1007/978-1-4614-8348-9_22. Videos can also be accessed at http://www.springerimages.com/videos/978-1-4614-8347-2

J.R. Samples, I.I.K. Ahmed (eds.), *Surgical Innovations in Glaucoma*,
DOI 10.1007/978-1-4614-8348-9_22, © Springer Science+Business Media New York 2014

many recent efforts have been directed towards new "blebless" procedures that do not rely on conjunctival placement and are less prone to these complications.

STARflo™ is a new glaucoma drainage device designed to provide a pathway for aqueous humor to travel from the anterior chamber into the suprachoroidal space, enhancing the natural uveoscleral outflow and eliminating the need for a filtering bleb. It is comprised entirely of Healionics' proprietary silicone STAR® Biomaterial, a precision-pore structure that creates a permanent multi-porous wicking system and that enhances biointegration and reduces fibrosis [7–9].

Background

The shape of the STARflo Glaucoma Implant is based on designs developed by Dr. Robert Nordquist in the 1990s [10, 11]. Originally based on cellulosic membrane, the material composition of the seton has evolved towards the use of a more advanced biomimetic structure and a more robust biocompatible material – the silicone STAR® Biomaterial manufactured by Healionics Corporation.

Cellplant Device

The use of setons to permanently lower IOP has been attempted for many decades. The first seton made of horsehair was implanted in 1906 to drain fluid out of the anterior chamber [12]. Since then, devices made from numerous other materials including silk thread, nylon, hydrogels, collagen, gold, platinum, silicones, and polythene have been described in the literature [13, 14]. Over time, these devices have varied widely in size, material composition, and design. In the 1990s, a novel approach was created by Drs. Robert Nordquist and Bing Li to overcome shortcomings that limit conventional aqueous tube shunts, such as foreign body reactions, inflammation, tube obstruction, and infection. Nordquist and Li described the material, the design, and the surgical protocol for a novel method of lowering the IOP [10, 11, 15, 16]. The material should exhibit certain characteristics for seton use:

- Biocompatible to avoid foreign body reaction, inflammation, and capsule formation
- Highly resistant to cellular attachment and invasion
- Nonabsorbable and stable at body temperature
- Pliable so as to fit the contours of the eye
- Soft enough to avoid scleral erosion, corneal irritation, inducement of undesirable changes in eye curvature, or damage to adjacent vasculature and tissue, but resilient enough to maintain shape and thickness
- Strong enough to keep the surgical fistula open permanently
- Porous so as to naturally regulates the flow of aqueous humor through the seton by mimicking the trabecular meshwork

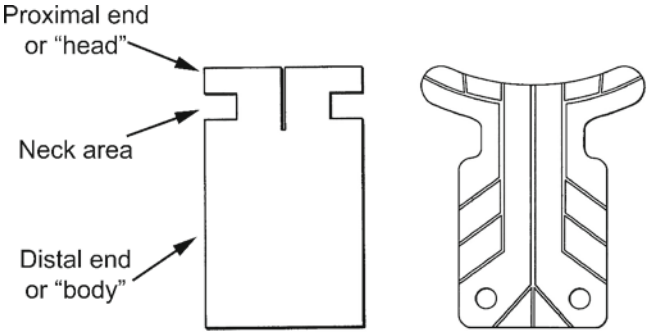

Fig. 22.1 Norquist's designs for seton use [11, 15]. Seton is comprised of a head, a neck, and a body portions. Further versions of the seton included grooved drainage channels, curved edges and proximal end, and suture holes

The multi-porous structure should also exhibit an inherent controlled resistance to flow first to prevent postoperative hypotony and second to regulate the rate of aqueous humor outflow proportional to the intraocular pressure. The material should also inhibit closure at the surgical site without producing inflammation, obstruction, or infection.

In the initial iteration, the seton devices were formed as thin flexible sheets with bottle-shaped profiles (Fig. 22.1). The proximal end ("head") extended into the anterior chamber and reduced to a narrow neck area passed through a limbal opening at the iridocorneal angle. The neck shape regulated the flow and securely held the seton in position. The distal end ("body") was rectangular shaped and entirely placed under a conventional 50 % thickness scleral flap. Typically, these setons were designed approximately 8–10 mm long with a width of 4–6 mm and a thickness of 50 μm. Some versions further included grooved drainage channels to facilitate increased ocular fluid flow from the anterior chamber, curved proximal ends to conform with the curvature of the anterior chamber, and suture holes in the body to secure the implant to the sclera.

The resultant "CELLplant" device (Fig. 22.2) was a filtering implant of similar shape to the first model shown on the left in Fig. 22.1 and made from the cellulosic membrane material widely used for hemodialysis filtering [10, 11]. This material exhibited many of the needed characteristics.

Toxicity, safety, and efficacy of the CELLplant device were successfully demonstrated in rabbits [10, 11]. In a first short study, the average IOP dropped from 22.0 to 14.3 mmHg in the eyes treated with the CELLplant device, whereas the control eyes treated with a normal filtering surgery had an average IOP of 20.2 mmHg after 70 days (p-value of 0.001). A 1-year study showed similar results with an average IOP reduction more than 30 % at the end of the experiment (Fig. 22.3). None of the rabbits developed corneal decompensation, conjunctival erosion, or uveitis as a result of the

implants. Scanning electron microscopy of the angle structures showed no evidence of corneal endothelial damage, iris atrophy, necrosis, or hypertrophy although there was iris touch. In all experimental eyes, except for one due to malposition of the implant, a functional filtering bleb was maintained, and the fistulas remained well open. Similar IOP results were also obtained in a cat with glaucomatous eyes.

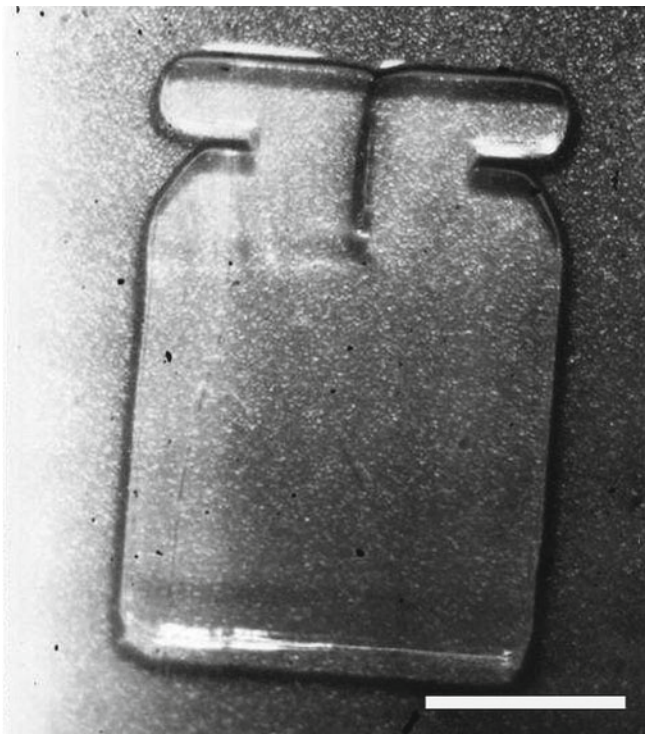

Fig. 22.2 Image of a hydrated CELLplant device. Once hydrated, CELLplant thickness was about 75 μm. *White scale bar* represents 3 mm (Used with permission of Dr. Robert Nordquist)

Based on the promising preliminary animal studies devoid of complications, a human clinical trial was conducted in the Republic of China in 1994–1995 by Dr. Li [10, 11, 17]. Twenty-three patients, exhibiting uncontrolled glaucoma of various type (neovascular, open angle, closed angle, traumatic) averaging over 60 mmHg of IOP and with previous failure to respond to conventional medical treatment, underwent filtration surgery with the CELLplant seton. The average IOP was 12 mmHg by the third-day postoperative, and all remained below 18 mmHg through 180 days. During the 24-month follow-up of the study (13 cases), no postoperative hypotony; complications including hyphema, uveitis, or infection; or flat chambers were observed, and the devices still functioned at the end of the study.

The feasibility of the surgical procedure and the promising results of the CELLplant device in significantly and sustainably dropping the IOP have been reported in both animal and human trials; further bench testing and an animal study on rabbits were conducted in response to the then newly issued (1998) US FDA Guidelines for Aqueous Shunts 510(k) (later issued as ANSI Z80.27-2001 Aqueous Shunts for Glaucoma Application) with the aim of commercializing the CELLplant device. Although IOP results correlated with those earlier observed (see Fig. 22.3), this animal study revealed certain issues of long-term fibrosis and mechanical fragmenting of the cellulosic material [18, 19]. The use of a more robust, long-term stable material was therefore required to overcome the drawbacks of the cellulose and to provide a future for Norquist's design. This material was found in the STAR® Biomaterial, invented at the University of Washington in 2003.

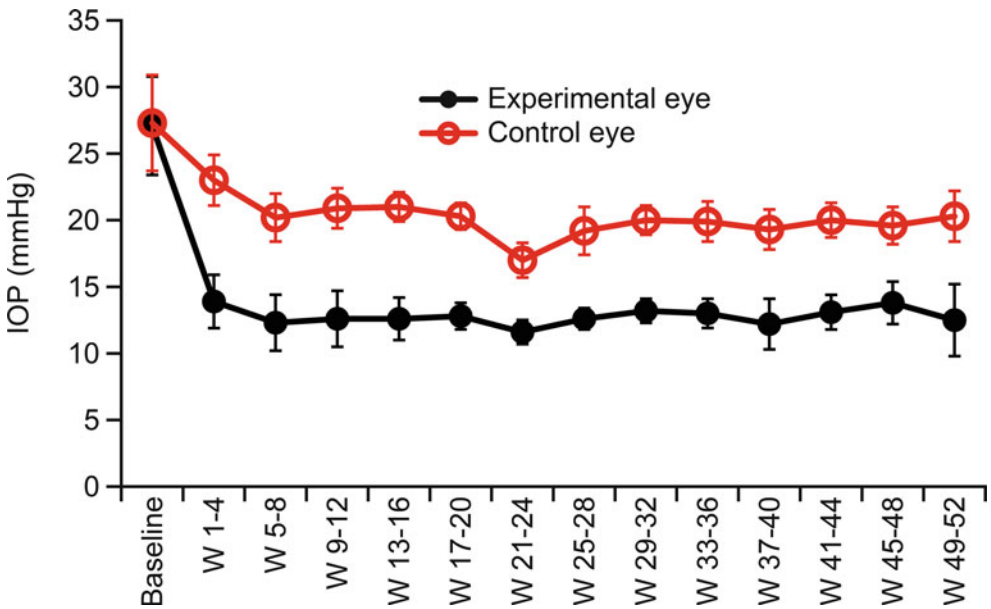

Fig. 22.3 One-year IOP follow-up in rabbits. For each animal (12 rabbits in total), one eye was implanted with CELLplant (experimental eye – *black line*) and the contralateral eye was used as control (open markers, *red line*)

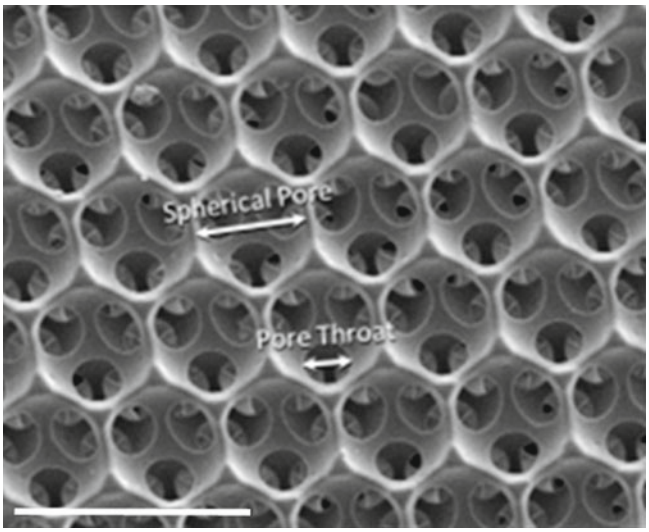

Fig. 22.4 SEM image of STAR® Biomaterial surface showing uniform dimensions of the pores and pore throats. *White scale bar* represents 50 μm

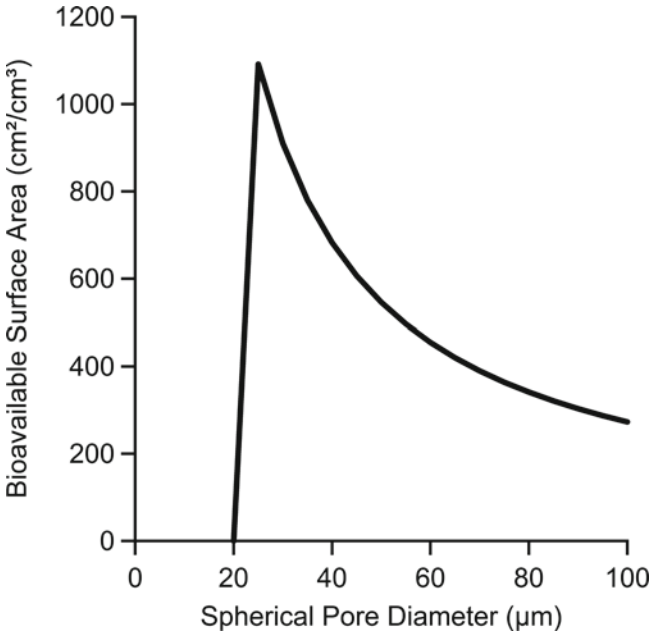

Fig. 22.5 Calculated bioavailable surface area for sphere-templated biomaterials as a function of the pore diameter. Note: calculations assume 40 % throat-pore size ratio, porosity of 65 %, 7.5 throats per pore, and 10-μm minimum throat size for cellular access [20]

STAR Material

Healionics' proprietary STAR® Biomaterial is a porous tissue engineering scaffold designed to promote healing of tissue around implanted medical devices with less scarring, improved vascularity, and a more stable long-term tissue-biomaterial interface.

A Precision-Pore Structure

STAR® Biomaterial contains a precisely controlled pore geometry made with a sphere-templating process developed at the University of Washington by Andrew Marshall and Buddy Ratner. Healionics has exclusively licensed patents from the University of Washington covering porous biomaterials with the optimized pore size for promoting vascular ingrowth and the sphere-templating methods for making them [7–9].

The sphere-templating process yields a pore structure with interconnected uniformly sized spherical pores. Since the size of the necks formed during the sintering step is carefully controlled, the size of the interconnections, or "throats," between the pores of the templated biomaterial is also precisely controlled. Figure 22.4 shows a scanning electron microscopy (SEM) image of the sphere-templated STAR® pore structure, with uniform dimensions of the pores and pore throats indicated. The ordered arrangement of the pores is an outcome of the fabrication method but is not believed essential to biological function so long as overall porosity and interconnection is maintained.

The pore size and structure of the STAR® Biomaterial are optimized for several biological effects that contribute the functionality of the STARflo™ Glaucoma Implant. These effects include maximized recruitment of macrophage cells into the pores, the subsequent vascularization of the implant with high capillary density, and the minimization of fibrotic scarring in the peri-implant tissues.

Maximized Macrophage Concentration

Macrophages are known to play a key role in the body's response to the tissue injury created upon implantation of a foreign biomaterial; these cells arrive at the tissue-biomaterial interface and attach to any exposed biomaterial surface area.

Pore structure of the STAR® Biomaterial is optimized so as to attract a maximized concentration of host macrophages into the pore structure. This is achieved by maximizing the surface area per unit volume available for macrophage attachment. As shown in Fig. 22.5, the so-called bioavailable surface area in the sphere-templated materials exhibits a sharp peak at the pore size of ~25 μm – the smallest pore size that allows macrophages to enter the spherical pores via the circular pore throats. Figure 22.6 demonstrates the sharp spike in macrophage concentration at 35 μm pore size, hence defining a "sweet spot" pore range between 25 and 35 μm represented by STAR® Biomaterial [21].

Beside the pore size, tight control of the pore throat diameter is also a critical parameter. On one hand, this dimension is on the same size scale as the macrophage cells (a human macrophage is 10–20 μm in diameter) [22]. To facilitate cellular infiltration, pore throats must therefore be at least ~10 μm in diameter. On the other hand, the throat-pore size

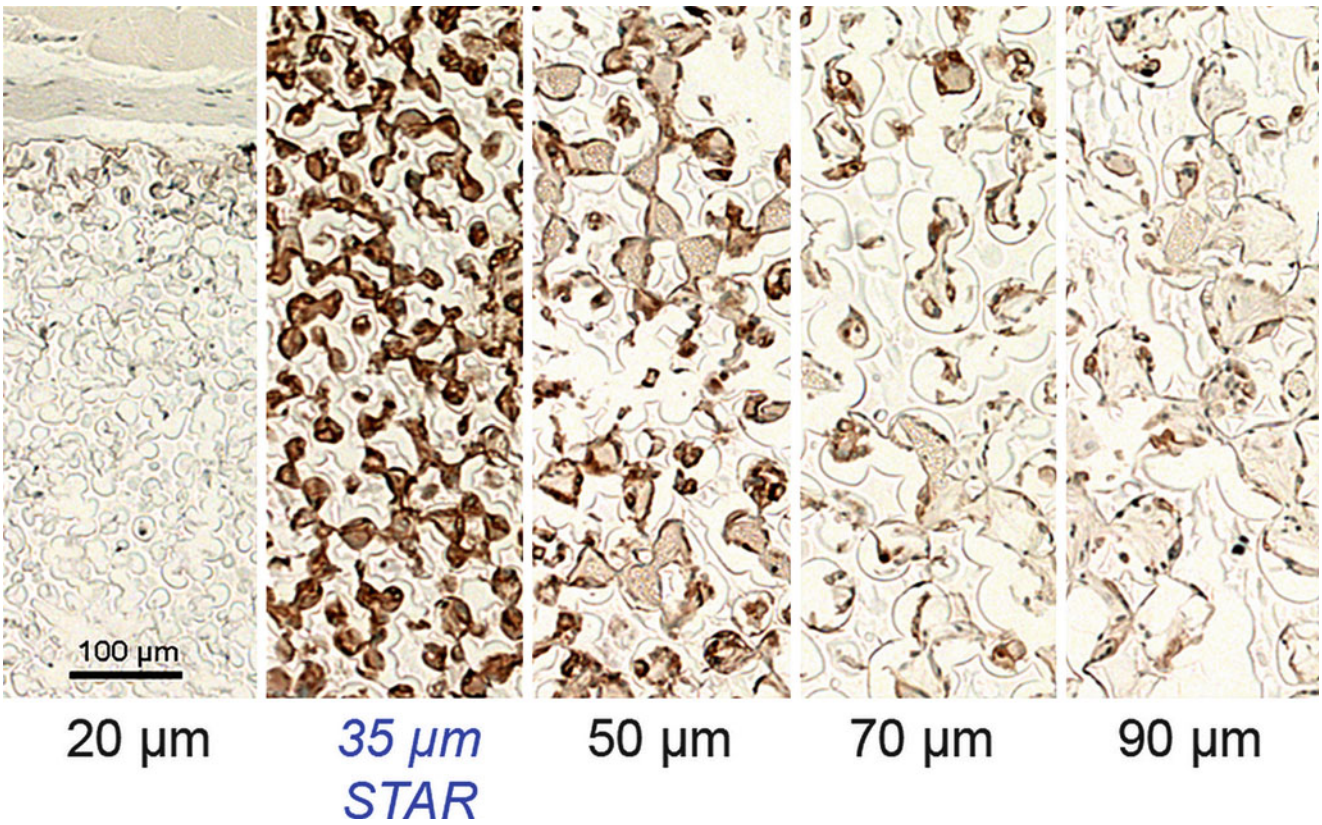

Fig. 22.6 Tissue sections of sphere-templated scaffolds with a series of controlled pore sizes implanted subcutaneously in mice for 4 weeks, stained with F4/80 macrophage marker. The 35-µm pore size (STAR® Biomaterial) is infiltrated with the largest number of F4/80 positive cells

ratio is constrained by practical considerations of the sphere-templated geometry: if the pore throat size is increased much beyond ~40 % of the spherical pore diameter, the neighboring pore throats within each pore would nearly overlap, and mechanical strength of the templated porous structure may fall off precipitously.

Maximized Vascularization

The STAR pore dimensions also encourage vascularization of the porous biomaterial with a robust capillary network. Figure 22.7 demonstrates that maximum blood vessel density occurs in the same "sweet spot" pore range of 25–35 µm and that the increased vascular density is observed not only within the pores but also in the capsule tissue immediately adjacent to the outer boundary of the porous implant [21]. The vascularizing effect mirroring the pore size dependent trend observed with macrophages suggests that the macrophages within the pores promote angiogenesis via the release of proangiogenic factors. The neovascularization effects of implanted porous biomaterials had been observed previously by other researchers [23, 24]. The precise dimensional control of the STAR® sphere-templating method allowed the optimum pore size for maximizing density of vascular ingrowth to be determined with greater accuracy. Since the method ensures all pores and

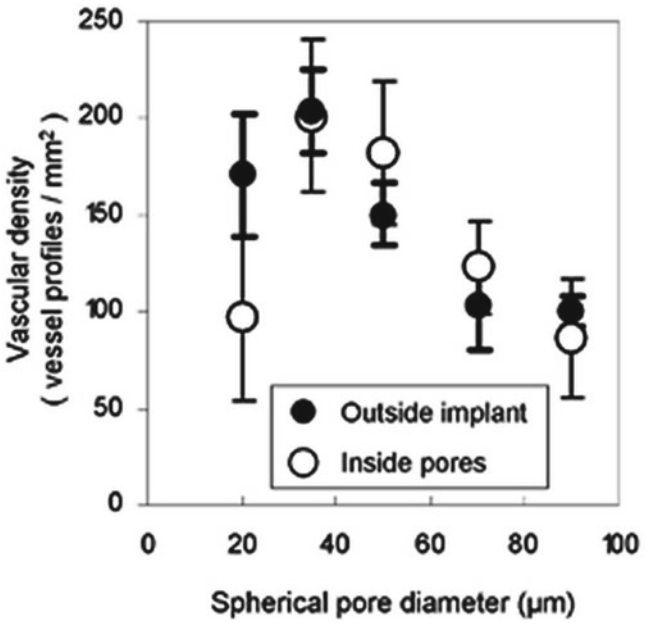

Fig. 22.7 In the "sweet spot" pore range around ~30 µm, the density of blood vessels is maximized both inside the implant and in the adjacent tissue within 50 µm of the implant. Vessels counted from sections of 4-week subcutaneous mouse implants stained with MECA-32 endothelial cell marker

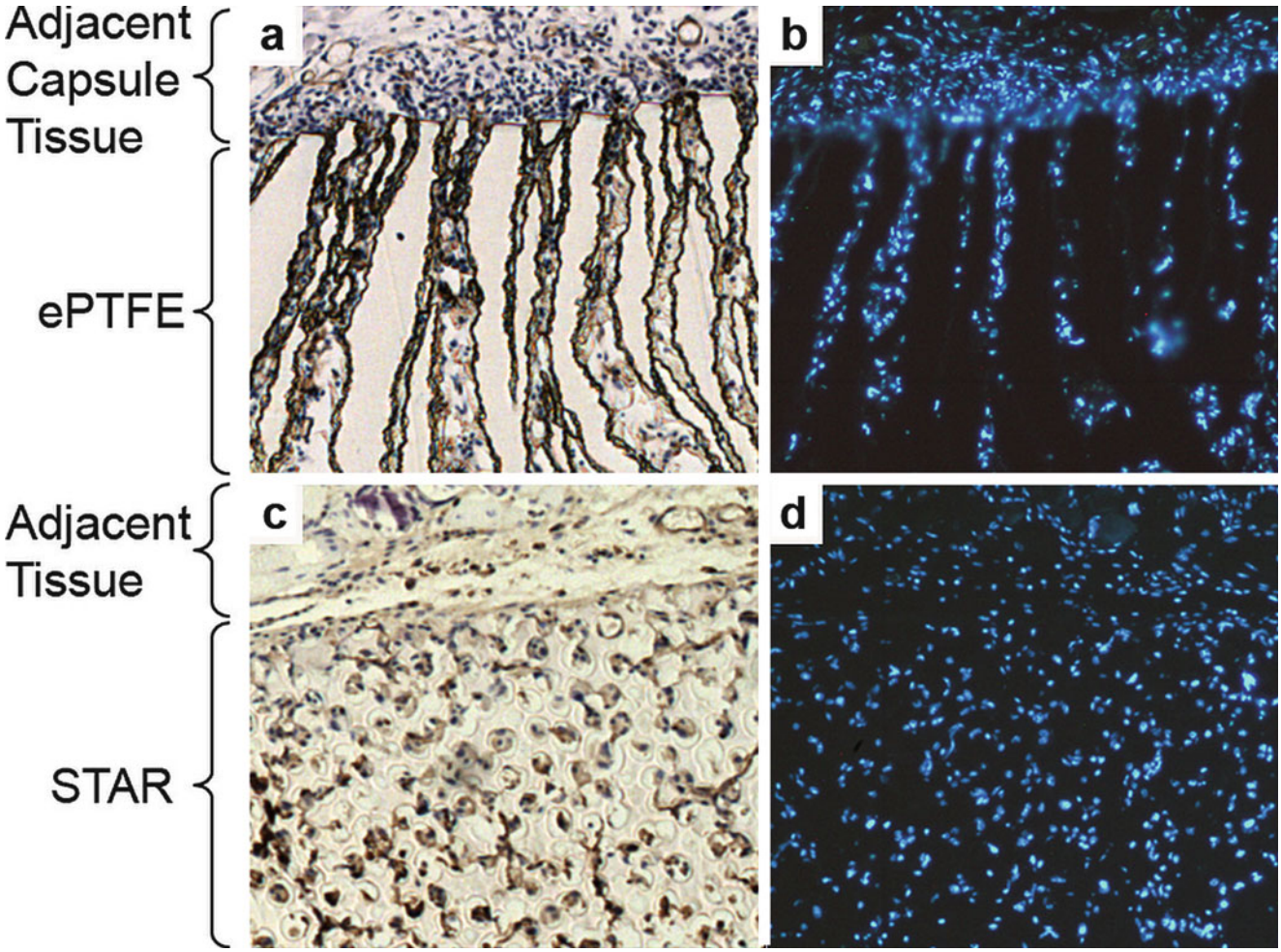

Fig. 22.8 Comparison of cellular integration at tissue-biomaterial interface for expanded polytetrafluoroethylene (ePTFE) (panels **a** and **b**) and STAR® Biomaterial (panels **c** and **d**). Tissue sections from scaffolds implanted subcutaneously in mice for 2 weeks, stained with MECA-32 brown endothelial marker (panels **a** and **c**) and with DAPI inflammatory cell nuclei marker (panel **b** and **d**). STAR material exhibits a more integrated interface with cells equally dispersed in scaffold and adjacent tissue while inflammatory cells accumulate and concentrate in adjacent capsule tissue around ePTFE implant (Used with permission of the authors and excerpted from [26])

pore throats in the structure are optimized in size, the localized proangiogenic effect is more pronounced.

The biointegration of STAR® Biomaterial was compared to expanded polytetrafluoroethylene (ePTFE) with 60-μm internodal distance – a porous biomaterial of similar pore size that has been investigated for glaucoma implants [25]. It was found that the STAR material induced a more smoothly integrated interface. As shown in Fig. 22.8, inflammatory cells accumulate in high concentration in the capsule tissue bordering the ePTFE implant, while the interface between the STAR® Biomaterial and the surrounding capsule tissue features a smooth transition in cellular density across the capsule-biomaterial boundary. Also, Fig. 22.9 shows that the endothelial cell concentration within the pores of STAR® Biomaterial was significantly greater than for ePTFE, indicating significantly increased intrapore neovascularization. The enhanced vascularizing effect compared to other porous biomaterials provided inspiration for the "STAR" acronym for sphere-templated angiogenic regeneration.

It has been hypothesized that the increased neovascularization associated with STAR Biomaterial could be attributed in part to a shift in macrophage polarity triggered when the spatially confined macrophages within the pore structure are directed by geometric cues towards a proangiogenic phenotype [27].

Anti-fibrotic Properties

Severalfold reductions in foreign body capsule thickness compared to nonporous controls have been observed for STAR Biomaterial in a variety of small and large animal models [21, 27, 28]. In Fig. 22.10, implant made from STAR® Biomaterial elicits remarkably thinner and looser foreign body capsule compared to nonporous control of same size and shape in a porcine subcutaneous implant model [28].

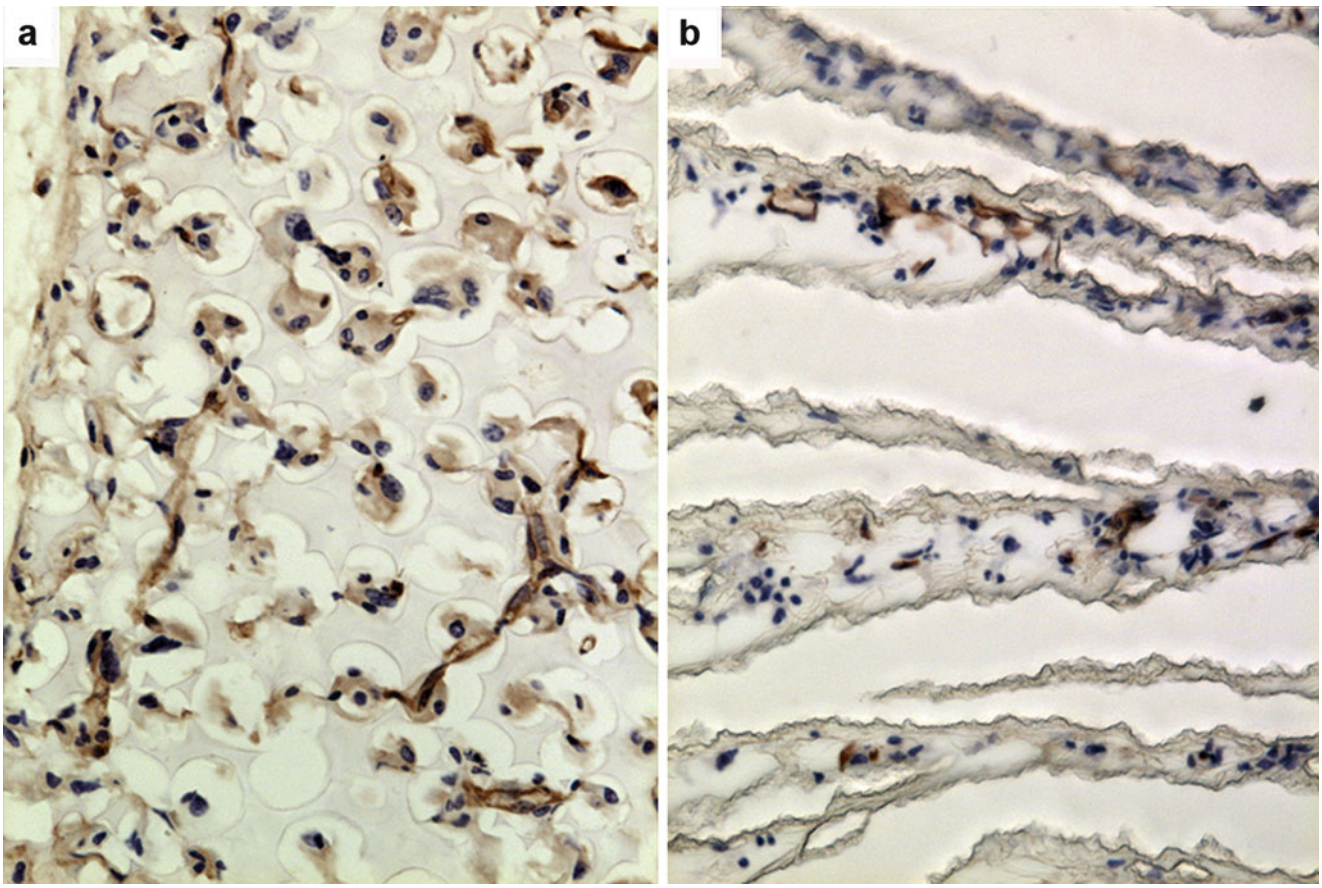

Fig. 22.9 Comparison of level of vascularization within STAR® Biomaterial and expanded polytetrafluoroethylene (ePTFE). Tissue sections from scaffolds implanted subcutaneously in mice for 2 weeks, stained with MECA-32 brown endothelial marker. STAR scaffold (panel **a**) shows much higher level of neovascularization than ePTFE (panel **b**) (Used with permission of the authors and excerpted from [26])

Although the mechanism for the reduction of peri-implant fibrosis is not fully understood, a plausible explanation is based on the idea that the vascularized tissue-biomaterial interface disrupts collagen lattice contraction. This "lattice slack" hypothesis is supported by a study where the capsule-reducing effects of STAR® Biomaterial were amplified by combining macrotopographic features and optimized microporosity in complementary configurations [28]. In that study, the absence of a myofibroblast layer in the capsule suggested a stress-relaxed condition with minimal fibrotic scar.

STAR Biomaterial's high resistance to fibrotic scarring represents a tremendous advantage for the STARflo device over other types of GDDs where fibrosis is a recurring problem in the sustainability of IOP-lowering efficacy.

STARflo Glaucoma Implant

Of similar shape to the CELLplant device, the STARflo™ Glaucoma Implant is entirely made from silicone STAR® Biomaterial. Besides meeting the specific physical characteristics defined by Nordquist, this biomaterial exhibits advantageous inherent properties for a glaucoma drainage device:

- The angiogenic properties are exploited by positioning the implant body in contact with the choroid, forming a well-integrated drain for the aqueous flow diffusing from the anterior chamber and minimizing the formation of a filtering bleb and its associated complication.
- The biomaterial's ability to reduce the thickness and density of the peri-implant fibrous capsule layer that forms during the course of the foreign body response may benefit longer-term pressure-lowering performance of the implant.

Material and Design

The STARflo device design is based on the previously mentioned patents. To overcome drawbacks associated with the cellulosic material of the CELLplant (e.g., long-term fibrosis and mechanical fragmentation), the STARflo device is made entirely from a long-term, implant silicone material (Nusil Technologies LLC, Carpinteria, USA) formed into the STAR

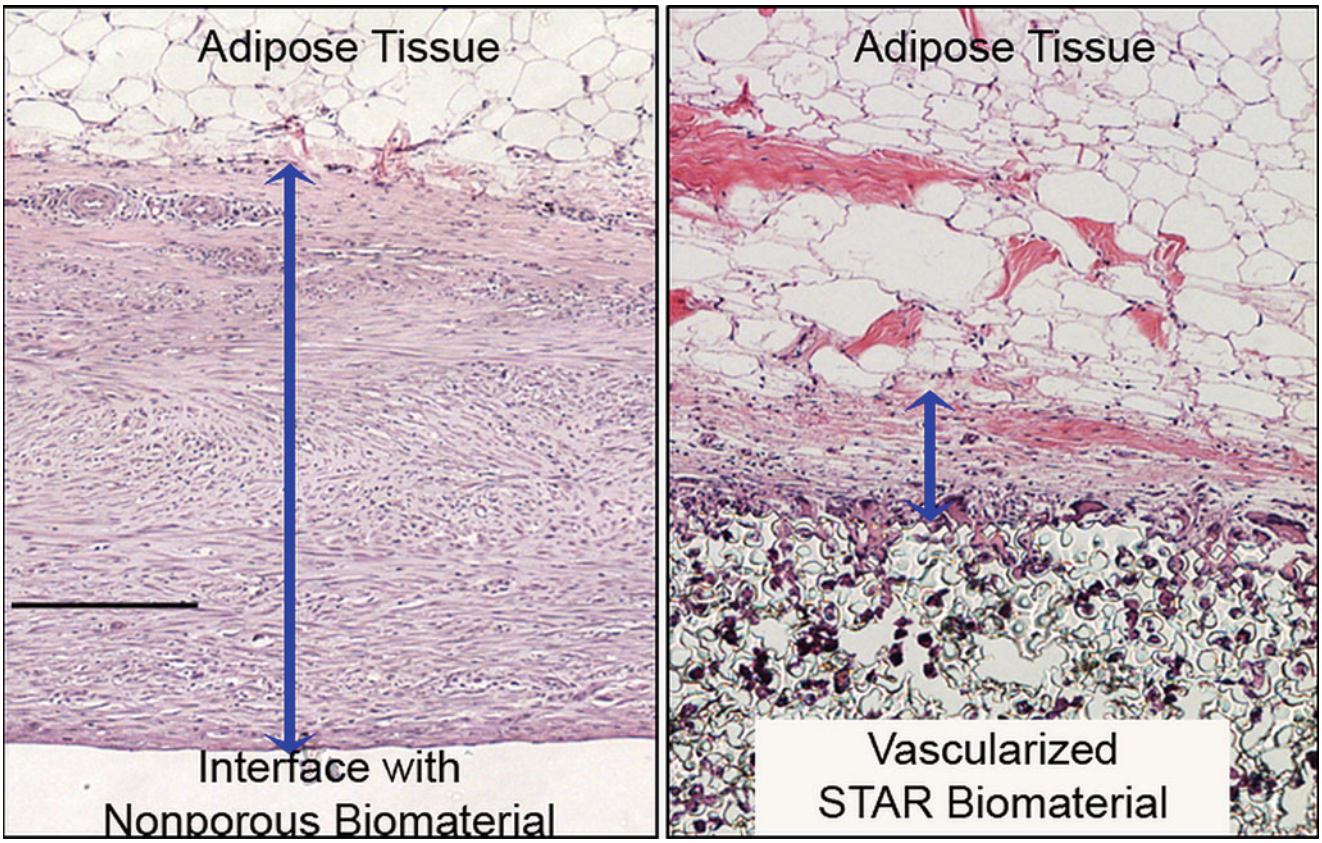

Fig. 22.10 H&E-stained tissue sections from 6-week subcutaneous porcine implants. *Blue bands* denote capsule thickness. The average thickness of capsules surrounding nonporous control implants (panel **a**) was nearly 4-fold greater than capsules surrounding STAR implants with 27-μm pore size (panel **b**). *Black scale bar* represents 200 μm

structure. Silicones exhibit superior mechanical properties, durability, and reduced inflammation in ophthalmic implants [29]. The device is made as a single continuous sheet of porous silicone STAR scaffold free from seams, joints, coatings, metal, or degradable substances. Pore size and throat size within the material are uniformly 27 and 9 μm, respectively, through the entire volume of the device (Fig. 22.11) and comprised within the "sweet spot" pore range. The device has the same length and width, and general shape as the CELLplant predecessor, but a nominal thickness of 300 μm. In use, most of the body sits in the suprachoroidal space.

The structure and pore dimensions of the STAR material forming the STARflo closely mimic those of the trabecular meshwork and the ~10-μm-sized natural drain openings into Schlemm's canal, making the head section mimic the normal drainage path.

Intended Use and Implant Location

The STARflo device is indicated for open-angle glaucoma. Implantation can be made in any location around the circumference of the globe providing that the rectus muscles are avoided. For ease of access and technical performance of the surgery, upper quadrants are the most commonly chosen location (1–2 o'clock (OS) or 10–11 o'clock (OD)).

Since the implant is entirely made from very soft porous silicone, the head area may be folded for ease of insertion to the anterior chamber via a small incision, just sufficient to retain the device neck. The anterior portion of the body then rests under a tight scleral flap while the posterior portion of the body is placed between the sclera and choroid (Fig. 22.12). This configuration provides a controlled fluid path for aqueous humor to drain from the anterior chamber to the suprachoroidal space of the eye. The implant bypasses the obstructed normal outflow passages and reduces the IOP without the need of a filtering conjunctival bleb prone to numerous complications. It also may spare patients wound healing issues associated with filtering surgery.

Surgical Procedure

The device is designed to be surgically placed in an *ab externo* fashion, under local retro- or parabulbar anesthesia. Because of its anti-fibrotic properties, STARflo implantation does not

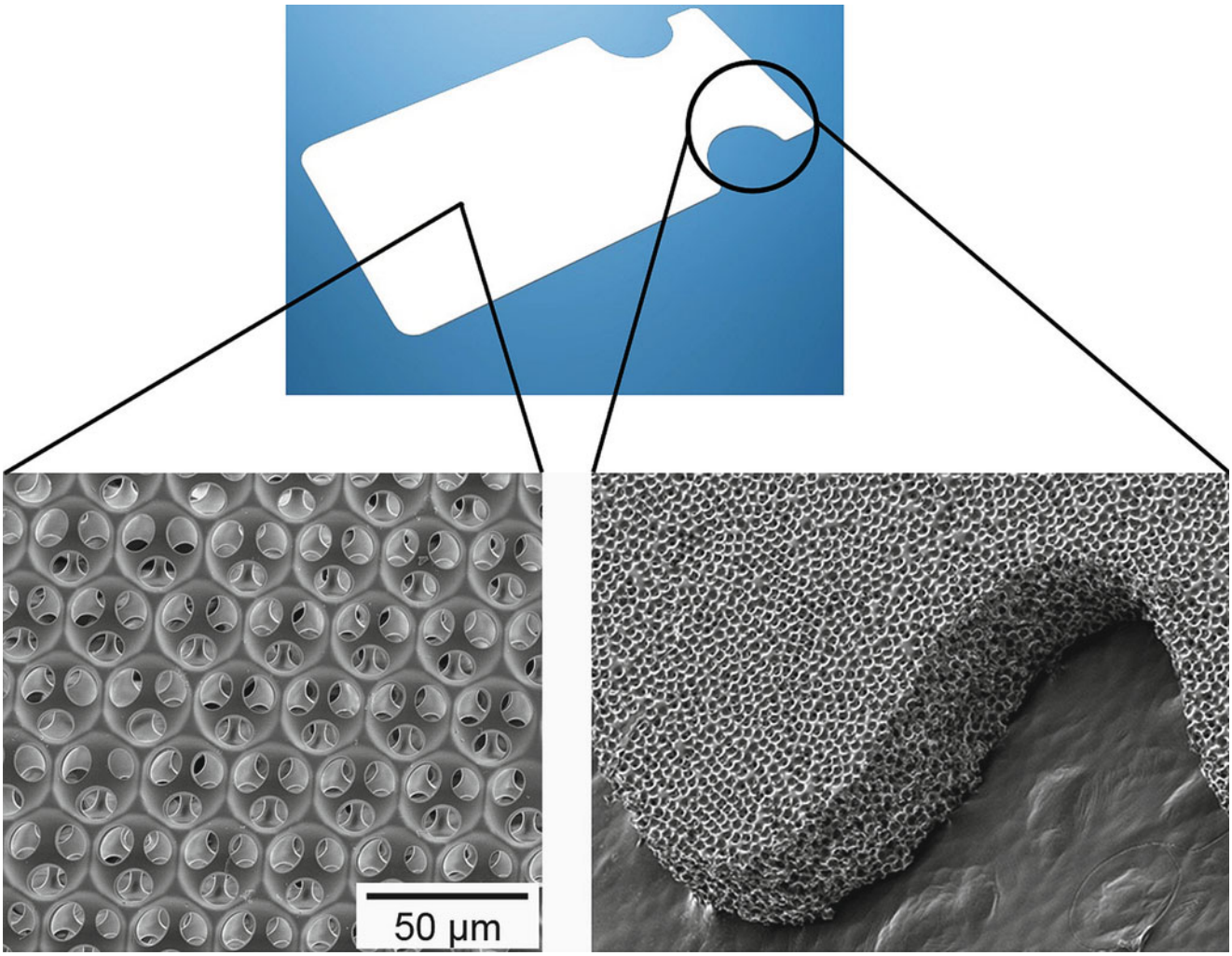

Fig. 22.11 SEM of the STARflo device entirely made of STAR® Biomaterial

require the use of anti-fibrotic agents such as mitomycin C (MMC) or 5-fluorouracil (5-FU). The surgical implantation procedure recommended by iSTAR Medical is animated in Video 22.1, although the choice of anesthesia and method or technique to implant the drainage device is upon surgeon discretion.

A fornix-based conjunctival peritomy is first created, followed by a superficial, rectangular scleral flap (50 % thick, 8 mm wide, 3 mm long) as depicted in Fig. 22.13a. The second layer of sclera is then cautiously incised to reveal the choroid tissue, parallel to the limbus and leaving a scleral bridge of 1–2 mm (Fig. 22.13b). A 3-mm-wide incision is performed to reach the anterior chamber through the trabecular meshwork and allows STARflo head to be introduced (Fig. 22.13c). A subscleral pocket is then created by separating the sclera from the choroid using a blunt spatula. The posterior aspect of the implant is gently guided into the suprachoroidal space (Fig. 22.13d). One corner of the STARflo head is then inserted into the anterior chamber through the previously created entry at the level of the scleral spur, followed by the other corner (Fig. 22.13e). When correctly placed, the implant neck is centered in the 3 mm incision and lays flat on the sclera without folds. The implant head is parallel to the iris to avoid incarceration or shunt-to-cornea touch and endothelial trauma. The scleral incision is then closed in a watertight fashion to avoid bleb formation. Finally, conjunctiva is sutured watertight. At all times, it is recommended to keep the implant moist using viscoelastic or sterile saline solution as a dry implant might compromise device performances. The use of non-toothed, blunt forceps is also recommended as well as avoidance of grasping the implant body.

Technical Characteristics

STAR® Biomaterial has a controlled and predictable resistance to fluid flow. The measured flow resistivity of the 27-µm-pore-sized STAR material is 0.08 mmHg/(µl/min).

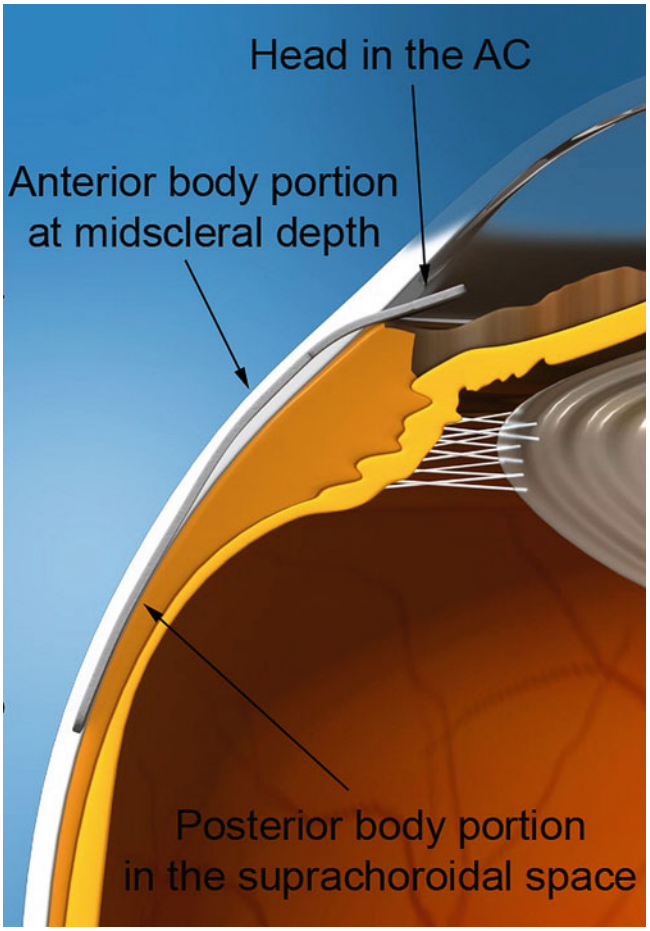

Fig. 22.12 Illustration of the anatomical placement of the STARflo device. The head of the implant is inserted in the anterior chamber, the anterior portion of the body rests under a scleral flap, and the posterior portion of the body is placed within the suprachoroidal space

For the specific shape of the STARflo device, modeling provides an estimated in vitro flow resistance of 0.4 mmHg/(µl/min) for aqueous transfer into the head section, through the neck and then dispersion from the body. This value is comparable to in vitro values for the well-established devices with tube connection between the anterior chamber and subconjunctivally located drainage plates. Under in vitro conditions, the device can convey 2.5 µl/min, equivalent to the normal aqueous inflow rate, with a pressure drop of 1 mmHg. In vivo, the natural differential in pressure between the anterior chamber and the suprachoroidal space permits the aqueous humor to drain through the STARflo device. STARflo does not rely on a subconjunctival bleb for IOP control, a well-known source of postoperative complications. However, formation of a small and transient bleb may be observed immediately after implantation, creating balancing back pressure to flow from the anterior chamber. Over time, as material integration with the choroid and sclera proceeds, it is hypothesized that infiltration of the STARflo pores by capillaries from the choroidal vasculature network provides enhanced fluid contact for stable fluid absorption from the eye.

Animal Study

Pre-market STARflo studies have been conducted on rabbits to assess safety in eye tissues and on dogs to assess performance in lowering IOP. At that time, implantation procedure recommended to create a full limbal-based scleral flap of the size of the implant body (8 mm in length by 6 mm in width) and to place the seton on the exposed choroid, followed by suturing the large scleral flap. Since then, STARflo surgery has evolved towards a trabeculectomy-like approach mainly to reduce risks of hyphema, choroidal prolapse, and choroidal hemorrhage.

Rabbit Study

A sponsored 6-month preclinical study was conducted on rabbits by NAMSA (Northwood, USA) to evaluate the ocular irritation and toxicity potential of the STARflo. The protocol, entitled "Ocular Irritation Study of STARflo Glaucoma Implant Following Implantation in the Anterior Chamber of the Rabbit Eye," followed the US FDA Guidelines for Aqueous Shunts 510(k) clearance. This study closely duplicated the rabbit study performed with the CELLplant device but with the substitution of the STARflo device [30].

In total, 14 non-glaucomatous rabbits were implanted with the STARflo Glaucoma Implant in one eye. For ease of surgery, the body of the device was positioned mid-scleral depth. Based on the results of ocular examinations, no ocular irritation or toxicity was associated with the implantation of the STARflo device.

Histology images at both 12 and 26 weeks showed a progression in tissue integration along the length of the implant from the anterior chamber to the intrasclerally placed posterior portion. In Fig. 22.14, the extent of the STARflo device from the anterior chamber (on the left) into sclera (on the right) is clearly observed. In enlargement Fig. 22.14a, pores of the device in the anterior chamber are acellular and open to flow. In limbus area (enlargement Fig. 22.14b), STARflo integration with adjacent tissue is observed without the formation of a fibrous capsule. The pores appear to contain fibroblasts. In the anterior scleral area (enlargement Fig. 22.14c), further away from the anterior chamber, some vascularized capsule is formed and pores are highly vascularized; macrophages surrounding the capillary structures are shown in high magnification in Fig. 22.15 [31]. In the

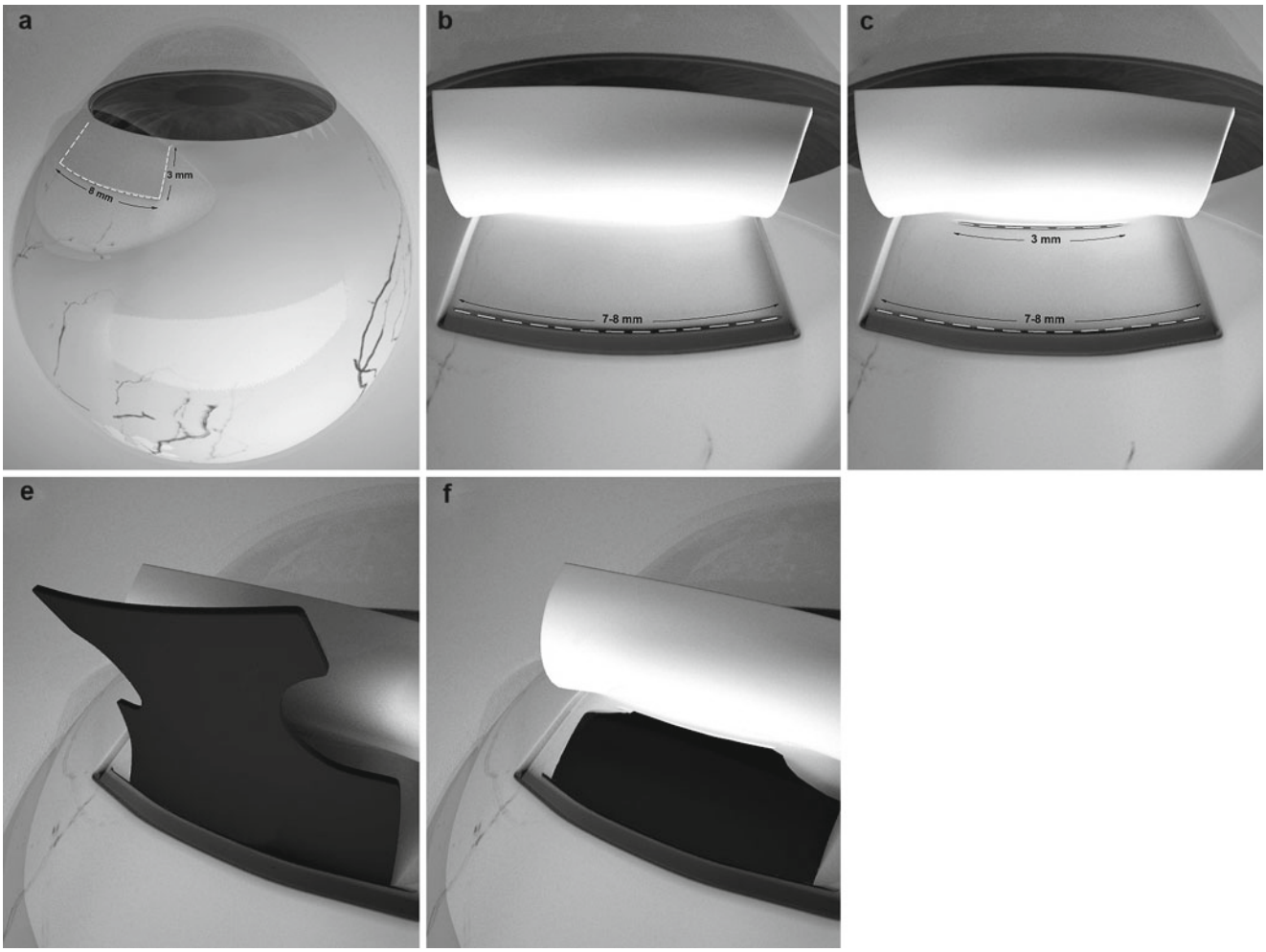

Fig. 22.13 Key sequences of the STARflo surgical procedure recommended by iSTAR Medical SA. A half-thickness scleral flap (8 mm wide, 3 mm long) is performed (panel **a**) followed by a posterior full-thickness scleral incision (panel **b**). A 3-mm-wide entry is created into the anterior chamber (panel **c**). Body implant is guided into the suprachoroidal space (panel **d**) while the head of the implant is inserted into the anterior chamber (panel **e**)

posterior scleral area (enlargement Fig. 22.14d), pores are also highly vascularized and populated with macrophages.

Histology images at 6 months also showed that a robust capillary network persists within the pores long term. These capillaries within the pores and within the capsule tissue immediately adjacent to the implant appear to provide the transport surface area for drainage of the aqueous fluid.

Those observations are similar to previous results on the STAR® Biomaterial implanted in other tissue areas and demonstrate that the STARflo device exhibits excellent biointegration properties with minimal fibrotic tissue interface formation [27]. The device exerts minimal stress on surrounding tissue and conforms to the anatomic shape of the eye due to its spongy, flexible, and soft structure, hence removing potential irritation and promoting fast healing of the incisions with minimum foreign body reaction.

Canine Study: The ClarifEYE

In collaboration with Dr. Craig Woods, CEO of TR BioSurgical, LLC (Chandler, Arizona), the STARflo device was initially introduced in 2008 for canine glaucoma veterinary use under the trade name ClarifEYE.

In a pilot study, glaucomatous dogs experiencing severe pain and unresponsive to maximum drug doses were implanted with ClarifEYE. Follow-up on two eyes over a 13-month period demonstrated that an IOP maintained between 10 and 20 mmHg after 1-year implantation (baseline IOP of 61.3 mmHg) and that needed medication could be decreased by 50 % [32]. The implant was observed to be well tolerated with minimal tissue reaction. To date, ClarifEYE has been implanted in more than 30 dogs of various breeds with glaucomatous eyes.

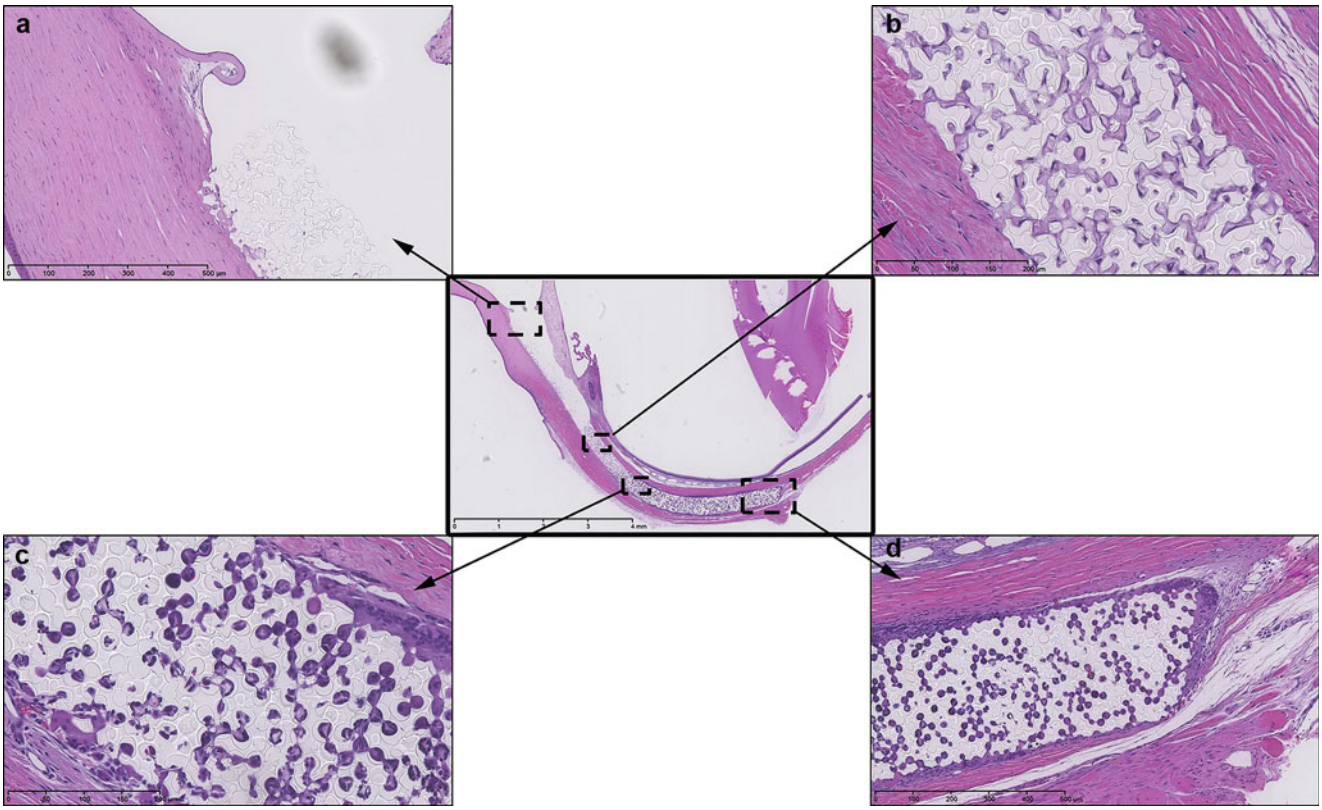

Fig. 22.14 Histology image and its enlargements taken 12 weeks after STARflo implantation within the sclera, H&E stain. In the anterior chamber, pores are acellular and open to flow (panel **a**). In limbus area, STARflo integration with adjacent tissue is observed without the formation of fibrous capsule (panel **b**). In the anterior sceral area, pores are highly vascularized (panel **c**). In the posterior scleral area, pores are also highly vascularized and populated with macrophages (panel **d**)

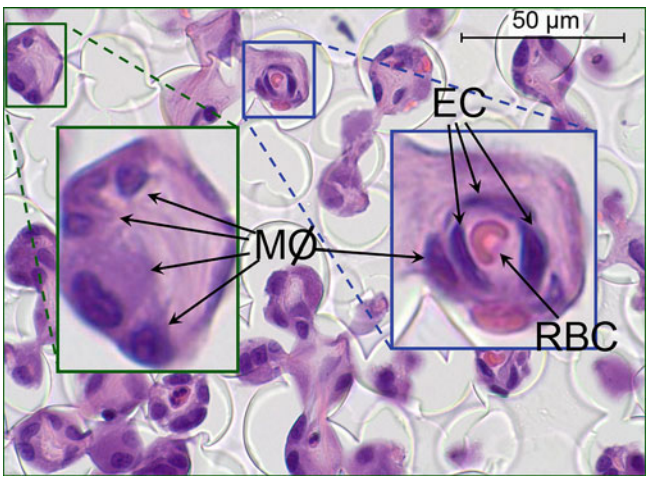

Fig. 22.15 Capillary network in STAR pores at 6 months for intrascleral implant in rabbit, with vascular endothelial cells (*EC*) surrounding red blood cell (*RBC*) and macrophages (*MØ*) lining the pore walls; H&E stain [31]

Human Clinical Study

A prospective, multicenter, feasibility trial was conducted to evaluate the safety and performance of the STARflo™ Glaucoma Implant in patients with open-angle glaucoma. This study started in June 2011 and will close after 12-month follow-up. The study took place in three clinical sites in Belgium.

Study Protocol

The aim of the study was to evaluate the safety of the STARflo Glaucoma Implant (i.e., implantation feasibility, incidence of device and procedure-related complications, and unanticipated adverse device effects) and its performance (i.e., reduction in IOP from preoperative baseline and reduction in number of glaucoma medications from preoperative baseline). The study protocol was approved by the respective ethics committees of the clinical sites. All patients signed an informed consent form to participate in the study.

The inclusion criteria for the clinical study were the following: (1) age of 18 years or older; (2) one or both eyes diagnosed with open-angle glaucoma or pseudoexfoliation glaucoma; (3) ability and willingness to return for up to 12 months of scheduled visits; (4) a documented IOP >21 mmHg in the study eye on medical therapy at two visits at least 48 h apart, within 2 months prior to study entry and at day of implantation; and (5) concurrent treatment with

ocular hypotensive medications in the study eye or prescription of anti-inflammatory and acetazolamide approximately 3 weeks before the surgery till 2 days before the surgery.

The exclusion criteria were (1) diagnosis of traumatic, uveitic, or active neovascular glaucoma; (2) previous surgery with any aqueous shunt device in the same eye quadrant; (3) clinically significant corneal disease (e.g., corneal dystrophy); (4) any previous ophthalmic surgery in the same eye quadrant other than trabeculectomy, trabeculoplasty, and cataract surgery within 3 months prior to study entry; (5) anterior chamber anatomic configuration of high risk for development of angle-closure glaucoma; (6) laser trabeculoplasty within 3 months prior to study; (7) active proliferative/inflammatory retinopathy; (8) clinically significant intraocular inflammation or infection within 6 months prior to study; (9) uveitis within previous 6 months before the surgery; (10) evidence of crystalline lens subluxation or luxation; (11) evidence of vitreous loss in the anterior chamber; (12) uncontrolled systemic disease (e.g., diabetes, hypertension); (13) pregnancy; (14) participation in any study involving an investigational drug or device within the past 3 months; and (15) intolerance or hypersensitivity to topical anesthetics, mydriatics, or components of the device.

Patient Follow-Up

Four patients (four eyes) with end-stage, medically uncontrolled IOP/refractory glaucoma were enrolled in this clinical study. Results for 6-month follow-up were collected to date.

First Patient

In 2011, a 43-year-old male consulted because of severe pain in the almost nonfunctional right eye and headache since 3 months. The patient was known with high intraocular pressure in the right eye (48 mmHg) for which he was treated with Cosopt and Travatan since 3 years. He was using a combination therapy – paracetamol and codeine – for his headaches nearly twice a week. In 1978, he had a limbal perforation resulting in a low visual acuity (+1 LogMAR) probably due to irregular astigmatism, followed by cataract extraction in 1988. His IOP began to rise in 2005. His visual acuity in his right eye was very low (>+1 LogMAR). Biomicroscopy showed a Binkhorst pupillary fixated IOL with iridectomy at 11 o'clock without any signs of inflammation. Fundoscopy showed an optic disc excavation of 0.9 and normal maculae. On gonioscopy, the angle was wide open. Glaucoma in the right eye might be related to low-grade subclinical chronic inflammation. The left eye was normal with an IOP of 17 mmHg.

Patient was implanted with STARflo in his right eye under retrobulbar anesthesia. Intraocular pressure in the implanted eye and medications prescribed during the study follow-up are listed in Table 22.1. Postoperative observations during this period were the following:

Table 22.1 IOP and medications for the first patient during the study follow-up

Visit	IOP (mmHg)	Medications
Surgery	48	Atropine
		Antibiotic and steroids
Day 1	2	Topical combination therapy of antibiotics/steroids
Week 1	5	Atropine
Month 1	29	
Month 2	29	
Month 3	38	Atropine was stopped spontaneously 3 weeks before the visit
		Antibiotics/steroids combination was continued
		Cosopt was started
Month 4.5	42	Cyclophotocoagulation (270°) → study discontinuation

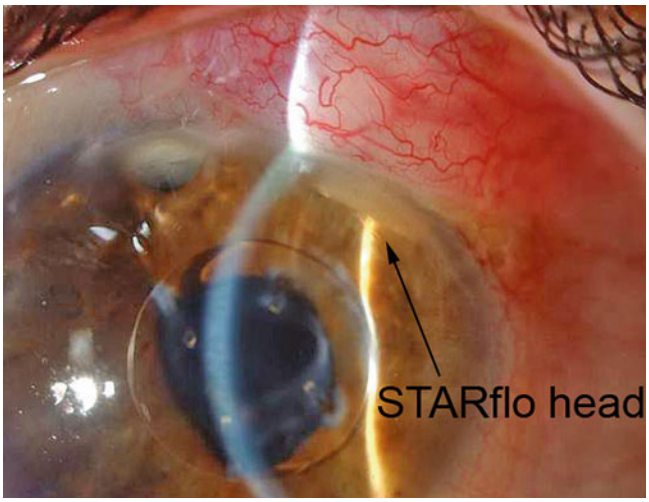

Fig. 22.16 Slit lamp image of the first patient taken 1 month postoperatively. The head of the STARflo is visible in the anterior chamber at the 1 o'clock position, not touching the iris or cornea

- Severe eye/headache pain resolved on the first-week postoperative visit, but mild headache without eye pain started 3 months after the surgery.
- Mild inflammatory postoperative reaction in the anterior chamber resolved within 1 month.
- Moderate conjunctival vascularization at the implant site.
- Mild conjunctival edema resolved within 3 months.
- No changes in the fundus during the follow-up.
- No signs of choroidal hemorrhage or retinal detachment.
- Visual acuity remained unchanged from baseline.
- Small subconjunctival bleb started to encapsulate at the first-month postoperative examination (Fig. 22.16) but disappeared at the 3-month visit.

At the 4.5-month visit, the patient was suffering from mild headache and photophobia, probably not related to the STARflo device, but the IOP rise (42 mmHg on the right eye

with Cosopt). The biomicroscopical scores remained unchanged. To reduce the IOP, a cyclophotocoagulation was performed (sparing the superonasal quadrant). At this point, the patient was discontinued from the study due to a lack of sufficient efficacy of the STARflo Glaucoma Device. After 10 days, a control visit showed an IOP of 10 mmHg in the right eye which slowly increased to 28 mmHg without pressure-lowering medication. Eleven months after the implantation, the STARflo device was removed because of persistent photophobia since the cyclodestruction, periocular pain, and conjunctival injection at the superonasal and inferior quadrants. The explant surgery went smoothly without any adverse event or complications. After a few days of hypotony, the IOP was again 24 mmHg 1 month after the explantation. Pain disappeared for a few months but relapsed afterwards. Photophobia was less, but not resolved. Six months after the removal of the implant, some anterior chamber inflammatory cells were seen for the first time, being a sign of chronic ocular inflammation. Probably a subclinical inflammation might have been the cause of the IOP rise from the start.

After this first implantation of STARflo in human, the surgical procedure was slightly adjusted based on surgeon's recommendation. The width of the superficial scleral flap and of the second layer of the sclera was assessed as too small (6 mm) for an easy implantation and for a watertight closure and was therefore increased to 7–8 mm for next surgeries.

Second Patient

A 56-year-old male consulted in 2011 because of severe eye pain. Cataract surgery was performed 3 years ago. Patient was diagnosed with primary wide open-angle glaucoma in the left eye since 4 years and was treated with Cosopt and Travatan. His right eye was normal. The visual acuity of the left eye was only light perception, and the IOP was 32 mmHg. The biomicroscopy showed a moderate conjunctival redness, a severe corneal edema with no inflammatory reaction in the anterior chamber. Fundoscopy showed a severe excavated optic nerve in the left eye. The patient was implanted with STARflo under general anesthesia. Key sequences of the implantation are available on Video 22.2.

IOP in the implanted eye and medications prescribed during the study follow-up are listed in Table 22.2. Postoperative observations during this period were the following:

- Ocular pain and pain sensation around the eye globe disappeared within 1 month postoperatively.
- Some diffuse conjunctival fluid was observed the day after the surgery.
- Severe, preoperative corneal edema decreased progressively and resolved on the 6-month postoperative visit.
- Moderate cells and trace of flare in the anterior chamber without signs of inflammation resolved within 2 months.

Table 22.2 IOP and medications for the second patient during the study follow-up

Visit	IOP (mmHg)	Medications
Surgery	32	Paracetamol Antibiotic
Day 1	2	Nonsteroidal anti-inflammatory drug (NSAID) Tropicamide Combination drops of antibiotics/steroids Antibiotic
Week 1	6	Paracetamol Tropicamide Combination drops of antibiotics/steroids NSAID
Week 2	26	Acetazolamide 250 mg was added because of signs of topical drug toxicity Antibiotic delivered in a single dose Steroid delivered in a single dose
Month 1	22	Steroid Antibiotic Acetazolamide 250 mg
Month 2	23	Steroids NSAID Antibiotic Acetazolamide 250 mg
Month 3	19	Acetazolamide 250 mg
Month 6	20	

- Small choroidal detachment was observed superiorly in the fundus, probably related to the surgical procedure, and resolved within 2 weeks.
- Diffuse bleb resolved within the first month after surgery.
- Visual acuity remained light perception.
- Preoperative cystoid macula edema decreased from grade 3 (severe) to grade 1 (mild) 2 months after the surgery.

Six months after the surgery, the overall situation remained satisfactory.

Third Patient

A 79-year-old female consulted in 2011 for an uncontrolled IOP in the left eye. The ophthalmological antecedents were congenital nystagmus and cataract surgery in both eyes. The patient was treated for primary open-angle glaucoma since 1994 in both eyes. Preoperatively, the eye pressure was 17 mmHg in the right eye and 29 mmHg in the left eye under Xalatan and Azopt. The visual acuity was only light perception in the left eye. Biomicroscopical exam revealed a mild corneal edema and a moderate corneal staining. The patient had abnormal macula and excavated optic nerve.

The patient underwent an operation with STARflo implant in 2011 in the left eye. The surgery was performed under general anesthesia. Intraocular pressure in the implanted eye and medications prescribed during the study follow-up are listed in Table 22.3. Postoperative observations during this period were the following:

Table 22.3 IOP and medications for the third patient during the study follow-up

Visit	IOP (mmHg)	Medications
Surgery	29	Antibiotic
		Steroids
		NSAID
Day 1	10	NSAID
Week 1	6	Cycloplegic drops
		Acetazolamide 250 mg is added because of peripheral choroidal detachment. Because of the conjunctival redness, an oral treatment was preferred to antihypertensive drops
		NSAID
Month 1	28	Xalatan
		Acetazolamide 250 mg (oral treatment) is preferred to eye drops because of the redness and conjunctival toxicity
		Combination drops of antibiotics/steroids
Month 2	26	Xalacom
		Combination drops of antibiotics/steroids
Month 3	18	Xalacom
Month 6	15	

- Calm anterior chamber.
- Ocular pain and discomfort, probably due to the surgery, resolved in 2 weeks.
- Mild conjunctival edema resolved within 2 week.
- Moderate conjunctival redness resolved within 1 month.
- Small bleb resolved within 1 month.
- No differences in the fundus from baseline.
- Small choroidal detachment was observed superonasally in the left fundus, probably due to the surgical procedure, and resolved within the first month.
- Visual acuity remained light perception although hand movement perception was reported on 1-month visit.

Six months after the surgery, the overall situation remained satisfactory.

Fourth Patient

A 83-year-old male patient from Morocco presented in 2011 because of progressive decrease of the vision especially in the left eye over 2 years. His ophthalmological history was blank. His visual acuity was + 0.12 LogMAR in the right eye and nearly +2 LogMAR in the left eye with his hyperopic correction. Slit lamp examination showed cataract in both eyes. The anterior chambers were slightly smaller than normal. Signs of exfoliation syndrome were observed on both lenses. The IOPs were 24 mmHg in the right eye and 37 mmHg in the left eye. Gonioscopy examination showed in both eyes a narrow angle in all the quadrants with a marked Sampaolesi's line. There were no visible posterior synechia in dynamic gonioscopy. In fundi after dilatation, a normal optic disc was observed with an excavation of 0.3 and normal rim in the right eye and a total excavation of the left optic nerve, C/D 0.9+ with an overall loss of rim. A peripheral iridotomy (PI) was performed as first treatment, and prostaglandins (PG) were prescribed. The IOP remained high despite of PI and PG treatment. A combination therapy Cosopt was added to PG. In 2011, the IOP was 23.5 mmHg in the right eye and 39 mmHg in the left eye.

Table 22.4 IOP and medications for the fourth patient during the study follow-up

Visit	IOP (mmHg)	Medications
Surgery	39	Steroid
Day 1	4	Antibiotic
Week 1	6	
Month 1	8	Antibiotics were stopped
		Steroids drops were continued because of the inflammatory reaction due to the exfoliative glaucoma and the combined procedure
Month 3.5	NA	Steroid drops were spontaneously stopped by the patient
Month 4.5	40	Cosopt was added
		Intensive topical steroid was added to tamper the inflammation of the anterior chamber
Month 6	14	Cosopt continued because of lack of persistency in medication use
		Intensive topical steroid

A combined operation, phacoemulsification cataract surgery first, followed by STARflo implantation, was performed on the left eye. Intraocular pressure in the implanted eye and medications prescribed during the study follow-up are listed in Table 22.4. Postoperative observations during this period were the following:

- Severe corneal edema and erosion, mainly caused by a complex cataract surgery, were resolved after 1 week.
- Small bleb resolved within 1 month.
- Merely due to the lack of compliance and the annulation of the third postoperative appointment by the patient, the following symptoms were observed 4.5 months after the surgery:
  - Signs of severe inflammatory reaction in the anterior chamber of the left eye resolved under intensive topical steroid drops.
  - Fibrin formation in front of the intraocular lens and on the STARflo head resolved on the 6-month postoperative visit.
  - Signs of synechia between the temporal angle of the STARflo head and the endothelium, still present on the 6-month visit but without disturbing the vision.
- Visual acuity slightly improved from +2.0 LogMAR to +1.2 LogMAR with postoperative correction.

On the 6-month postoperative control, the patient had neither complains nor pain even touching the site of operation.

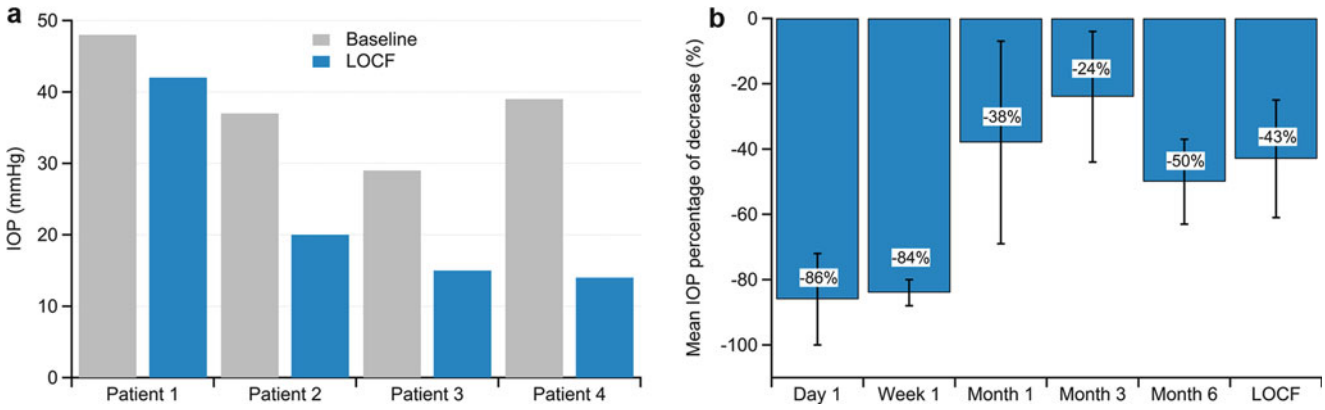

Fig. 22.17 Comparison of IOP per patient at baseline and LOCF (panel **a**) and mean IOP percentage decrease at visit time (panel **b**). Patient 1 was discontinued after 4.5 months. *LOCF* last observation carried forward, e.g., at 4.5 months postoperatively for patient 1 and 6 months for patients 2, 3, and 4

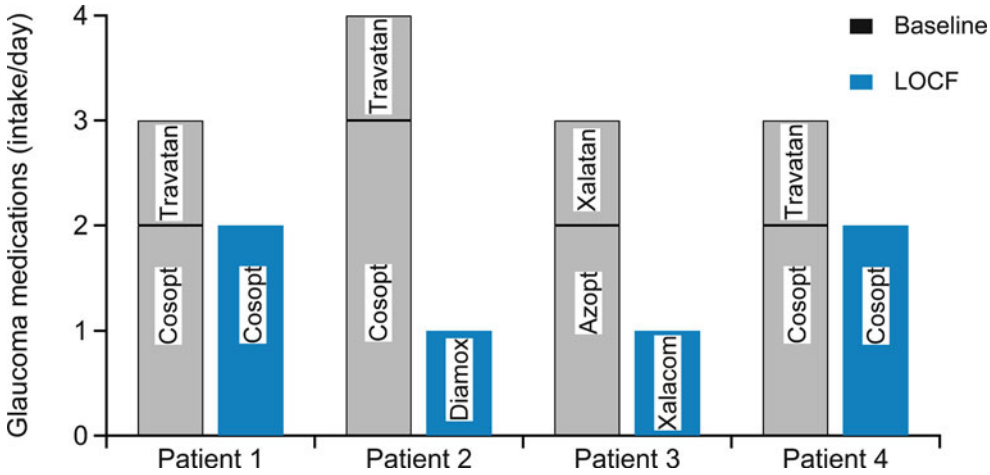

Fig. 22.18 Comparison of glaucoma medication per patient at baseline and LOCF (last observation carried forward, e.g., 4.5 months postoperatively for patient 1 and 6 months for patients 2, 3, and 4)

Clinical Trial Summary

From a clinical perspective, the 6-month results of the STARflo clinical study showed that all the safety and the efficacy endpoints were achieved:

- For all patients, the STARflo implantation procedure was feasible without adverse events during or immediately after surgery.
- No device-related adverse events were reported.
- Transient choroidal detachment was encountered in two patients and probably procedure related, which resolved within the first month after surgery.
- Transient hypotony (IOP < 6 mmHg) resolved within 1 week in three patients and within 1 month in one patient.
- Postoperative bleb was seen in all four patients and disappeared between 1 week and 3 months.
- After 6-month follow-up (three cases), mean IOP percentage of decrease was 50 %, and an IOP < 21 mmHg was reported for all three patients still in study at that time (Fig. 22.17).
- After 6-month follow-up (three cases), the mean daily intake of glaucoma medication decreased by 60 % (Fig. 22.18).

However, despite the fact that a mean decrease in IOP and IOP-lowering medications was reported, no statistical significance between baseline and the last observations can be claimed due to the limited size of the studied cohort.

Concerning the first implanted patient whom been dropped out of the study, the scleral flap of 6 mm in width was too small to obtain watertight closure and was related to a more sustained filtering bleb (filtering up to 1 month, encapsulated bleb up to 3 months). Whether this might be related to an insufficient STARflo efficacy in lowering IOP remains an open question. STARflo devices placed in subsequent patients were inserted using a larger incision, and each exhibited a transient bleb and satisfactory IOP-lowering efficacy. On the other hand, this eye had probably a chronic low-grade inflammation which is a known risk factor for early fibrosis and failure in all filtering procedures.

Conclusion

STARflo Glaucoma Implant is a new suprachoroidal drainage device that combines Nordquist's designs and the unique biointegration properties of the STAR® Biomaterials to enhance the natural uveoscleral outflow, hence reducing the intraocular pressure without the formation of a filtering bleb and its associated complication.

The STARflo device relies on extensive research and studies conducted for several years on the STAR® Biomaterial as implantable material and on STARflo predecessors in the ophthalmic field – the CELLplant and the ClarifEYE. In the ophthalmic field, the safety and the performances of the STARflo device were demonstrated on animals while early results on human shows encouraging results in the control of the IOP with a reduction of glaucoma medications. Although long-term success still has to be demonstrated, this newly CE-marked device exhibiting anti-fibrotic properties is promising as a novel, suprachoroidal implant for bleb-free, intraocular pressure reduction for patient suffering from refractory open-angle glaucoma. iSTAR Medical SA is currently running a controlled market rolled-out phase during which each new case is carefully followed.

Acknowledgments The authors express warm thanks to M. Maginness (PhD, Healionics Corporation), Dr. R.E. Norquist (PhD, Wound Healing Of Oklahoma, Inc.), and Dr. C. Woods (DVM, BioVeteria Life Sciences, LLC) for their contribution and inputs in this chapter.

References

1. Bill A, Philips CI. Uveoscleral drainage of aqueous humor in human eye. Exp Eye Res. 1971;12(3):275–81.
2. Toris CB, Yablonski ME, Wang YL, Camras CB. Aqueous humor dynamics in the aging human eye. Am J Ophthalmol. 1999;127(4):407–12.
3. Weinreb RN. Uveoscleral outflow: the other outflow pathway. J Glaucoma. 2000;9(5):343–5.
4. Weinreb RN, Toris CB, Gabelt BT, Lindsey JD, Kaufman PL. Effects of prostaglandins on the aqueous humor outflow pathways. Surv Ophthalmol. 2002;47 Suppl 1:S53–64.
5. Mosaed S, Minckler DS. Aqueous shunt in the treatment of glaucoma. Expert Rev Med Devices. 2010;7(5):661–6.
6. Boyle JW, Netland PA. Incisional therapies: shunts and valved implants. In: Schacknow PN, Samples JR, editors. The glaucoma book – a practical, evidence-based approach to patient care. New York: Springer; 2010. p. 813–30.
7. Ratner BD, Marshall A, inventors; University of Washington, assignee. Porous biomaterials. United States patent US 7972628 B2, 5 July 2011.
8. Ratner BD, Marshall A, inventors; University of Washington, assignee. Crosslinked porous biomaterials. United States Patent US 8318193, 27 Nov 2012.
9. Ratner BD, Marshall A, inventors; University of Washington, assignee. Novel porous biomaterials that support vascular ingrowth. European Patent EP 1670385, 23 Jan 2013.
10. Nordquist RE, Li B, inventors; Wound Healing of Oklahoma, assignee. Method and apparatus for lowering the intraocular pressure of an eye. United States Patent US 5704907, 6 Jan 1998.
11. Nordquist RE, Li B, inventors; Premier Laser Systems Inc., assignee. Method and apparatus for lowering the intraocular pressure of an eye. United States Patent US 6102045, 15 Aug 2000.
12. Rollet M, Moreau M. Traitement de l'hypopyon par le drainage capillaire de la chambre antérieure. Rev Gen Ophthalmol (Paris). 1906;25:481–9. French.
13. Hong C-HH, Arosemena A, Zurakowski D, Ayyala RS. Glaucoma drainage devices: a systematic literature review and current controversies. Surv Ophthalmol. 2005;50(1):48–60.
14. Luntz MH, Harrison R. Alloplastic devices in glaucoma surgery: setons. In: Lim ASM, series editor. Glaucoma surgery. Singapore: World Scientific; 1994. p. 153–63.
15. Lisk JR, Memmen JE, Hampton SM, Nordquist RE, Robledo PV, Tai M-K, inventors; Medtronic-Xomed INc, assignee. Article and method for ocular aqueous drainage. United States Patent US 7160264 B2, 9 Jan 2007.
16. Lisk JR, Memmen JE, Hampton SM, Nordquist RE, Robledo PV, Tai M-K, inventors; Medtronic-Xomed Inc., assignee. Device for ocular aqueous drainage. European Patent EP 1578319B1, 23 Jan 2010.
17. Sabbagh L. Early results good with glaucoma seton. Ophthalmol Times. 1995;20(40):10–2.
18. Intraocular Implantation Study in the Rabbit. NAMSA study protocol and report # 02T0101300, 2002.
19. Martson M, Viljanto J, Hurme T, Laippala P, Saukko P. Is cellulose degradable or stable as implantation material? An in vivo subcutaneous study in the rat. Biomaterials. 1999;20(21):1989–95.
20. Marshall AJ, Ratner BD. Quantitative characterization of sphere-templated porous biomaterials. AIChE J. 2005;51(4):1221–32.
21. Marshall A. Hydrogels with well-defined pore structure for biomaterials applications. PhD dissertation, University of Washington; 2004: AAT 3151637.
22. Krombach F, Münzing S, Allmeling AM, Gerlach JT, Behr J, Dörger M. Cell size of alveolar macrophages: an interspecies comparison. Environ Health Perspect. 1997;105 Suppl 5:1261–3.
23. Brauker JH, Carr-Brendel VE, Martinson LA, Crudele J, Johnston WD, Johnson RC. Neovascularization of synthetic membranes directed by membrane microarchitecture. J Biomed Mater Res. 1995;29(12):1517–24.
24. Sharkaway AA, Klitzman B, Truskey GA, Reichert WM. Engineering the tissue which encapsulates subcutaneous implants. II. Plasma-tissue exchange properties. J Biomed Mater Res. 1998;40(4):586–97.
25. Bae HB, Kim CS, Ahn BH. A membranous drainage implant in glaucoma filtering surgery: animal trial. Korean J Opthalmol. 1988;2:49–56.
26. Terasaki D, Sobel M, Irvin C, Wijelath E, Ratner BD. Biomaterial-Induced Angiogenesis To Adress Peripheral Vascular Disease: The Application of Sphere Templated Hydrogels. In: Scholz C, Kressler J, editors. Tailored polymer architectures for pharmaceutical and biomedical applications. ACS Symp Ser 2013. p. 245–57.
27. Madden LR, Mortisen DJ, Sussman EM, Dupras SK, Fugate JA, Cuy JL, et al. Proangiogenic scaffolds as functional templates for cardiac tissue engineering. Proc Natl Acad Sci U S A. 2010;107(34):15211–6.
28. Marshall AJ, Alvarez M, Maginness M, inventors; Healionics Corporation, assignee. Implantable medical devices having microporous surface layers and method for reducing foreign body response to the same. United States Patent US 2011/0257623 A1, 20 Oct 2011.
29. Ayyala RS, Michelini-Norris B, Flores A, Haller E, Margo CE. Comparison of different biomaterials for glaucoma drainage devices: part 2. Arch Ophthalmol. 2000;118(18):1081–4.
30. Ocular Irritation Study of STARflo glaucoma implant following implantation in the anterior chamber of the rabbit eye. NAMSA study protocol and report # 10T5296802, 2010.
31. Biotechnol Bioeng. 2012;109(8):C1.
32. Roberts S, Woods C. Preliminary report: effect of a novel porous implant in refractory glaucomatous dogs. In: Veterinary ophthalmology. Abstracts: 39th annual meeting of the American College of Veterinary Ophthalmologists, Boston, 15–18 Oct 2008, p. 423.